CHEMICAL ENGINEERING TRANSACTIONS
VOL. 94, 2022
A publication of AIDIC
The Italian Association of Chemical Engineering
Online at www.cetjournal.it
Guest Editors: Petar S. Varbanov, Yee Van Fan, Jiří J. Klemeš, Sandro Nižetić

ISBN 978-88-95608-93-8; **ISSN** 2283-9216
DOI: 10.3303/CET2294077

Influence of Geometry and Mechanical Load on the Delamination in the Graphene/Polymer Nanocomposite Under Axial Load

Apostol Apostolov[a,*], Elisaveta Kirilova[a], Rayka Vladova[a], Natasha Vaklieva-Bancheva[a], Tsvyatko Rangelov[b]

[a] Bulgarian Academy of Sciences, Institute of Chemical Engineering, Acad. G. Bonchev str., Bl.103, Sofia 1113, Bulgaria
[b] Bulgarian Academy of Sciences, Institute of Mathematics and Informatics, Acad. G. Bonchev str., Bl.8, Sofia 1113, Bulgaria
a_apostolov@iche.bas.bg

This paper presents a theoretical study on the influence of the geometry (layer thickness and length) and the magnitude of axially applied tension load on the delamination in a three-layer graphene/PMMA nanocomposite. Two different analytical solutions (Case 1 and Case 2) for the interface shear stress in the middle layer of the nanocomposite structure are obtained, based on the application of a two-dimensional stress-function method and minimization of the strain energy. The theoretical criterion for delamination in the interface layer, which is based on the model interface shear stress, is formulated. The obtained non-linear equation with respect to debond length is solved numerically, for both solutions, at different values of the mechanical load and geometry of the structure layers. For both solutions, it was found that the magnitude of the applied tension load influences strongly the appearance of delamination in the structure. For Case 1 (thinner PMMA layer) the delamination could be observed over 350 MPa external load; for Case 2 (thicker PMMA) it could be seen over 750 MPa. If the structure length decreases, under the above-mentioned conditions, the delamination begins at slightly lower values of the tension load. The magnitude of the applied load influences also the value of debond length. The obtained results could be used for fast prediction of safety intervals of applied loads and geometry design (without delamination) in similar nanocomposite devices to assure their safety working as sensors, nano- and optical electronic devices, energy devices, etc.

1. Introduction

It's been 17 y since graphene was discovered by Novoselov et al. (2005). From that moment the world of material science is changing constantly, because of the unique graphene structure – a two-dimensional (2D) atomic crystal and its very surprising properties: Young's modulus of 1 TPa; intrinsic strength of 130 GPa; very high thermal conductivity (above 3,000 W mK^{-1}); optical absorption of about 2.3 % (in the infrared limit); complete permeability to any gases. It can sustain extremely high densities of electric current (on the order of 10^6 times higher than copper) as is reported by Novoselov et al., (2012). The chemical functionalization of graphene leads to the creation of new nanoscale materials. For example, Nair et al., (2010) synthesized fluorographene - a two-dimensional counterpart of Teflon; it has high thermal and chemical stability, also a great insulating ability just like its macroscale analogue. In the work of Loh et al., (2010) the chemistry and reactivity of graphene where different molecules are bonded to the carbon monolayer crystal are described. Another application of graphene is to graphene-polymer composites, which can be used in mechanics, electronics, medicine, packaging, chemical industries and environmental protection. An implementation of the graphene nanocomposites is their use as additives in the production of supercapacitors according to Cheng, (2015). The graphene nanocomposite could be used as a material for the removal of lead ions (Pb^{2+}) from water as shown in the work of Thy et al., (2020). Graphene oxide membranes (Zunita et al., 2020) could be used also for metal ions removal from industrial wastewater. The addition of graphene and copper to epoxy resin has shown significant improvement in mechanical properties, thermal stability and heat resistance of the

Paper Received: 15 April 2022; Revised: 10 June 2022; Accepted: 16 June 2022
Please cite this article as: Apostolov A., Kirilova E.G., Vladova R.K., Vaklieva-Bancheva N.G., Rangelov T., 2022, Influence of Geometry and Mechanical Load on the Delamination in the Graphene/ Polymer Nanocomposite Under Axial Load, Chemical Engineering Transactions, 94, 463-468 DOI:10.3303/CET2294077

obtained nanocomposite (Li et al, 2017). Despite the wide applications of graphene, currently, there is no complete life cycle assessment (LCA) on nanomaterials or nanotechnology reported in the literature. Only a few studies present limited evaluation based on Life Cycle thinking (Mata et al., 2015).
As it can be seen from the review of Dhand et al, (2013) and all mentioned above, graphene and its derivatives like graphene nanocomposites have a great potential use. Implementation of the nanomaterials requires the theoretical and practical research of the mechanical properties of the nanocomposite structure, as well as how it works and react to the applied loads, which geometric dimensions are most appropriate, in order to determine the optimal dimensions and loads at which the structure could work without destruction. Experimentally, it was found that the proper choice of the length of the graphene flakes in the nanocomposite (more than 10 μm) is crucial for the prevention of debonding in the structure (Anagnostopoulos et al., 2019).
Nowadays, the finite elements commercial software and molecular modelling (Rahman and Haque, 2013) has a wide application for simulation of nanocomposites behaviour. But there are only few analytical models that can describe on macro level the behaviour of the layered nanocomposites under combined loading, and as was commented in Gong, (2012), their main drawback is that most of them are one-dimensional (shear-lag). In our previous works (Kirilova et al., 2019) and most recent (Petrova et al., 2022) analytical modelling of the two-dimensional stresses in the three-layered nanocomposite is proposed, based on the two-dimensional stress-function method and minimization of complementary strain energy functional. In the available literature, only the influence of the graphene flake length on the efficient reinforcing in graphene-polymer nanocomposites is investigated - for graphene/poly(methyl methacrylate) (PMMA) in Androulidakis et al., (2019) and for graphene/ Polyethylene terephthalate (PET) in Xu et al., (2016). In both these papers it was done combining shear-lag model calculations and experimental measurements for determine the interface shear stress. The influence of other geometric dimensions and magnitude of applied load in the nanocomposite on the delamination are not studied.
To eliminate the gap between the theory and experimental data, this paper's focus is set on the modelling of delamination in a graphene/polymer nanocomposite subjected to static extension load and determining the factors that influence on it. Using two different geometries for the layer's thicknesses and a parametric analysis, the influence of magnitude of applied load and of the length of the nanocomposite structure on the delamination is modelled and investigated. The safety intervals for preventing nanocomposite structure from delamination in respect to applied load and geometry (thickness and length) are determined.

2. Statement of the Problem and Developed Analytical Solutions

The representative volume element (RVE) of nanocomposite – graphene monolayer/SU-8/PMMA, which is shown in Figure 1 will be examined in this study. The axial tensile force P (N·m) is applied to the PMMA layer. The coordinate system *Oxy* is placed at the left end of the structure with a length l, the y-coordinates for the layers are: $b = h_2, c = h_2 + h_a, y_t = h_2 + h_a + h_1$. In the work of Kirilova et al. (2019), a detailed description and development of two-dimensional stress function method for axially loaded nanocomposite structure graphene/SU-8/PET, is presented. In (Petrova et al., 2022) the same method is applied for the structure shown in Figure 1 and the other type of solution, different from that in (Kirilova et al., 2019) is developed. Here, for the case of brevity only model assumptions, few of the equations and the two solutions are given.

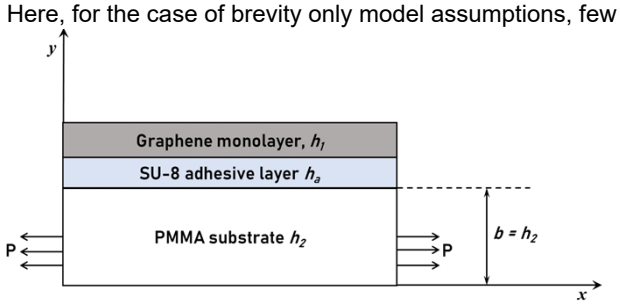

Figure 1: Scheme of the three-layer nanocomposite structure

The initial assumptions of 2D stress-function variation method for the considered nanocomposite structure consist in the following:
1. The axial stresses in the layers are assumed to be functions of axial coordinate x only. Physically, no load transfer occurs over the layers ends.
2. In the adhesive interface layer the axial stress $\sigma_{xx}^{(a)} \equiv 0$ is neglected.

3. All stresses in the layers (axial, normal (peel) and shear stresses) are determined under the assumption of the plane stress formulation (standard constitutive strain-stress equations from 2D elasticity theory).
According to Petrova et al., (2022), Eqs. (1) and (2) give the two dimensional stresses $\sigma_{xx}^{(i)}$, $\sigma_{xy}^{(i)}$, $\sigma_{yy}^{(i)}$ in each layer $(i=1,2,a)$ of the nanocomposite structure, which are expressed in terms of a single stress potential function (the axial stress of the graphene layer is noted with σ_1, function only of *x*) and its first and second derivatives:

$$\sigma_{xx}^{(1)}=\sigma_1(x)=\sigma_1,\qquad \sigma_{yy}^{(1)}=\frac{1}{2}(y-y_t)^2\sigma_1^{"},\qquad \sigma_{xy}^{(1)}=(y_t-y)\sigma_1^{'} \tag{1}$$

$$\sigma_{xx}^{(a)}\equiv 0,\qquad \sigma_{yy}^{(a)}=\left[\frac{h_1^2}{2}+h_1(c-y)\right]\sigma_1^{"},\qquad \sigma_{xy}^{(a)}=h_1\sigma_1^{'} \tag{2}$$

$$\sigma_{xx}^{(2)}=\sigma_0-\rho\sigma_1,\qquad \sigma_{yy}^{(2)}=\frac{-\rho}{2}\left[y^2-y(y_t+h_a)\right]\sigma_1^{"},\qquad \sigma_{xy}^{(2)}=\rho y\sigma_1^{'},\quad \text{where}\quad \rho=\frac{h_1}{h_2} \tag{3}$$

Application of two-dimensional stress-function method and minimization of complementary strain energy result is Eq.(4) - a 4th order differential equation, in respect to the axial stress of graphene layer σ_1, with constant coefficients D_i. The latter (Eqs. 4-9) depend on the layers thicknesses and their material properties as Young module and Poisson ratio, also on the magnitude of the applied static tensile load - $h_i, E^{(i)}, \nu^{(i)}, \sigma_0$.

$$2D_2\sigma_1^{IV}+(2D_3-2D_4)\sigma_1^{"}+2D_1\sigma_1+D_5=0 \tag{4}$$

$$D_1=\frac{h_1}{E^{(1)}}+\frac{h_2\rho^2}{E^{(2)}} \tag{5}$$

$$D_2=\frac{h_1^5}{20E^{(1)}}+\frac{h_1^2h_2}{120E^{(2)}}\left[6h_2^2-15h_2(y_t+h_a)+10(y_t+h_a)^2\right]+\frac{h_1^2h_a}{12E^{(2)}}\left[3h_1^2+6h_1h_a+4h_a^2\right] \tag{6}$$

$$D_3=-\frac{\nu^{(1)}h_1^3}{3E^{(1)}}-\frac{\rho\nu^{(2)}h_1h_2\left[2h_2-3(y_t+h_a)\right]}{6E^{(2)}} \tag{7}$$

$$D_4=\frac{2}{3}\frac{(1+\nu^{(1)})h_1^3}{E^{(1)}}+\frac{2}{3}\frac{(1+\nu^{(2)})}{E^{(2)}}h_1^2h_2+\frac{2(1+\nu^{(a)})h_1^2h_a}{E^{(2)}} \tag{8}$$

$$D_4=\frac{2}{3}\frac{(1+\nu^{(1)})h_1^3}{E^{(1)}}+\frac{2}{3}\frac{(1+\nu^{(2)})}{E^{(2)}}h_1^2h_2+\frac{2(1+\nu^{(a)})h_1^2h_a}{E^{(2)}} \tag{9}$$

$$D_5=-\frac{2h_2\rho\sigma_0}{E^{(2)}} \tag{10}$$

As is shown in Petrova et al., (2022), the homogeneous Eq. (4) has a characteristic equation of fourth order in respect to unknown stress function σ_1. The corresponding quadratic equation discriminant can be positive or negative, so its roots can be real, complex or mixed. The sign of this discriminant depends on the thicknesses and material properties of the structure layers, e.g. from coefficients $D_i, i=1\div5$, but not depend on the external tensile load $\sigma_0=P/h_2$. The last one is included in the solutions for σ_1 in our previous works. After determining of the function σ_1 and it's derivatives, all the stresses in the structure layers can be obtained, using the Eqs. (1-3). The axial stress in the graphene layer (the general analytical solution in the case (noted here as Case 1) of four real roots λ_i (Petrova et al., 2022), and its first derivative are presented by:

$$\sigma_1=C_1\cdot\exp(\lambda_1\cdot x)+C_2\cdot\exp(\lambda_2\cdot x)+C_3\cdot\exp(\lambda_3\cdot x)+C_4\cdot\exp(\lambda_4\cdot x)-A \tag{11}$$

$$\sigma_1^{'} = C_1 \cdot \lambda_1 \exp(\lambda_1 \cdot x) + C_2 \cdot \lambda_2 \exp(\lambda_2 \cdot x) + C_3 \cdot \lambda_3 \exp(\lambda_3 \cdot x) + C_4 \cdot \lambda_4 \exp(\lambda_4 \cdot x) \quad (12)$$

Eqs. (13) and (14) present the general solution in the case (noted here as Case 2) of complex roots $\alpha \pm i\beta$ and its first derivative (Kirilova et al., 2019):

$$\sigma_1 = \exp(-\alpha x)[M_1 \cos(\beta x) + M_2 \sin(\beta x)] + \exp(\alpha x)[(M_3 \cos(\beta x) + M_4 \sin(\beta x)] - A \quad (13)$$

$$\begin{aligned}\sigma_1^{'} = {} & \exp(-\alpha x)[M_1(-\alpha\cos(\beta x) - \beta\sin(\beta x)) + M_2(\beta\cos(\beta x) - \alpha\sin(\beta x))] + \\ & + \exp(\alpha x)[(M_3(\alpha\cos(\beta x) - \beta\sin(\beta x)) + M_4(\alpha\sin(\beta x) + \beta\cos(\beta x))]\end{aligned} \quad (14)$$

The constant $A = D_5/2D_1$ is the solution for non-homogeneous Eq. (4) and depends on external static load and C_i and M_i are integration constants in the model solutions, determined from respective boundary conditions. The delamination in the structure depends on the value of interface shear stress (ISS) in the adhesive layer, namely $\sigma_{xy}^{(a)} = h_1\sigma_1^{'}$. If this shear stress is greater than ultimate shear stress in the adhesive layer SU-8 (30 MPa), the delamination takes place for some values of external load and geometry dimensions of the construction. Having both solutions and their first derivatives, it is easy to obtain the model interface shear stress in both cases. A theoretical non-linear equation for length of debonding in the structure is presented:

$$\sigma_{xy}^{(a)}(x) = \sigma_{USS}^{(a)} \quad (15)$$

where $\sigma_{USS}^{(a)}$ is the ultimate shear strength of the adhesive. The value of x for which Eq. (15) holds, is the debond length of delamination. Graphically, it represents the intersection of the interface shear stress curve $\sigma_{xy}^{(a)}$ with the straight horizontal line corresponding to $\sigma_{xy}^{(a)} = \sigma_{USS}^{(a)}$ (the value for the ultimate shear strength).
A parametric analysis is made in the next section, where for each of the obtained ISS solutions and fixed values for the geometrical parameters, the following parameters can be changed: σ_0 - the value of the axial load; l - the length of the RVE; h_2 - the height of the substrate layer; h_a - the height of the adhesive layer. The aim of this analysis is to obtain safety intervals for geometry and external load for the structure, for which no delamination occurs.

3. Results and discussion

The geometrical and mechanical characteristics of the considered nanocomposite structure (Figure 1) graphene flake/SU8/PMMA, are: $l = 12 \cdot 10^{-6}\,\text{m}$, $E^{(1)} = 1 \cdot 10^{12}\,\text{Pa}$, $E^{(2)} = 3.5 \cdot 10^{9}\,\text{Pa}$, $E^{(a)} = 2 \cdot 10^{9}\,\text{Pa}$, $v^{(1)} = 0.13$, $v^{(2)} = 0.35$, $v^{(a)} = 0.22$, unless the other is stated. The layer's thickness (given in Table 1) is connected to the model solution for ISS of Case 1 (real roots) – Eq. (12) and Case 2 (complex roots) – Eq. (14). All calculations of ISS are performed in developed Mathcad Prime programs, the graphics were built in Sigma Plot, v.13. Here, the discriminant of quadratic equation and its roots are given in Table 1 together with the geometry configuration in the layers for two Cases.

Table 1: Geometry configuration for calculated model solutions for interface shear stress in adhesive layer of nanocomposite structure

Case	h_1,m	h_a,m	h_2,m	Discriminant for quadratic equation	Roots of quadratic equation
Case 1	0.35×10^{-9}	1×10^{-8}	2×10^{-6}	4.38×10^{24}	1.333×10^{13} ; 1.123×10^{13}
Case 2	0.35×10^{-9}	4×10^{-8}	1×10^{-5}	-3.681×10^{24}	$(4.942 \times 10^{11}) \pm i\,(9.593 \times 10^{11})$

The parametric analysis is performed for both solutions for ISS in Table 1. First, the magnitude of applied static tension load was varied, for fixed values of the material properties and geometry as they were defined. The influence of magnitude of external load on the interface shear stress for Case 1 is shown in Figure 2. The same procedure was repeated for Case 2 to investigate the effect of different thicknesses of layers on the ISS. For both Cases the length of the structure is fixed at 12 μm.

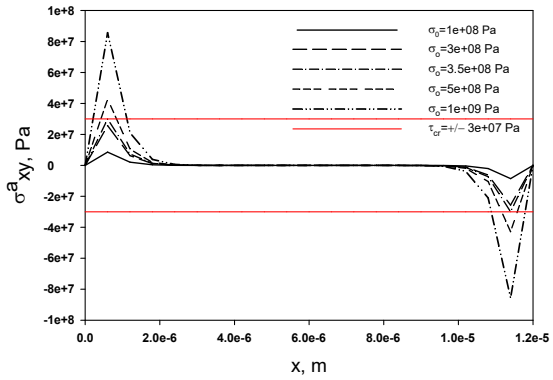

Figure 2: Influence of the magnitude of applied mechanical load σ_0 on the interface shear stress in adhesive layer, for Case 1 solution

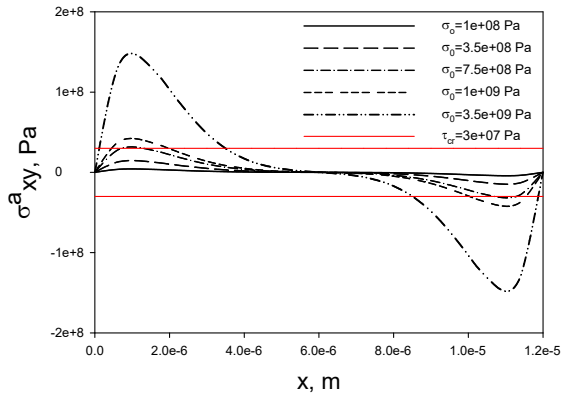

Figure 3: Influence of the magnitude of applied mechanical load σ_0 on the interface shear stress in adhesive layer, for Case 2 solution

The following result is obtained for Case 1: if $\sigma_0 \geq 350$ MPa, then a delamination of the graphene layer occurs, which is visible from the fact that graphically ISS are larger than the critical value for adhesive – 30 MPa (red line in Figure 2). The value of calculated debond length by Eq. (15) for the maximal applied load (3.5 GPa) is about 1.5 μm. For the ISS at Case 2, from the parameters presented, will give: if $\sigma_0 \geq 750$ MPa, then a delamination of the graphene layer will occur. The value of calculated debond length by Eq. (15) for the maximal applied load (3.5 GPa) for Case 2 is about 3.5 μm. These results for debond lengths coincide very well with experimentally obtained data for interface shear stress of (Anagnostopoulos et al., 2019) for the graphene/SU-8/PMMA.

The other part of the parametric analysis is connected with the influence of length structure on the delamination in it. Four different structure lengths (from 6 to 30 μm) were tested to analyse influence of the geometrical parameters of the substrate layer and to determine the critical magnitude of the applied load, after which a delamination will occur. The results are presented in Table 2.

Table 2: Critical magnitude of applied load, over which delamination appears for various structure lengths

Case	l =6 μm	l = 12 μm	l = 20 μm	l = 30 μm
Case 1	$\sigma_0 \geq 2.5 \times 10^8$ Pa	$\sigma_0 \geq 3.5 \times 10^8$ Pa	$\sigma_0 \geq 8.5 \times 10^8$ Pa	$\sigma_0 \geq 3.3 \times 10^9$ Pa
Case 2	$\sigma_0 \geq 7.5 \times 10^8$ Pa	$\sigma_0 \geq 7.5 \times 10^8$ Pa	$\sigma_0 \geq 7.2 \times 10^8$ Pa	$\sigma_0 \geq 8 \times 10^8$ Pa

It can be concluded for Case 1, that delamination depends strongly on the structure length and occurs at higher loads with length increasing. This is confirmed by the experimental observation of Gong (2012) for the efficient stress transfer for graphene flakes >30 μm. For Case 2 (thicker structure) practically, there are no influence of the length on the critical load after which delamination takes place.

4. Conclusions

The parametric analysis over the influence of the geometry (layer thickness and length) and the magnitude of axially applied tension load on the delamination in a three-layer graphene/SU-8/PMMA nanocomposite structure is performed. Based on the model solutions for all stresses in the structure considered, the model ISS in the middle adhesive layer is calculated for different geometry of the structure (Case 1 and Case 2) and different magnitudes of the applied load. It was found that safety intervals (without delamination in the structure) with respect to loading could be fixed up to 350 MPa for thinner Case 1 and up to 750 MPa for thicker Case 2. The values of debond lengths are determined in both Cases by the proposed non-linear equation for ISS and coincide well with those reported in the literature. The length of the structure influences the delamination for thinner Case 1 significantly; for thicker geometry (Case 2) it is not essential.

Acknowledgments

The authors gratefully acknowledge the Bulgarian National Science Fund for its financial support via the contract for project КП-06-Н57/3/15.11.2021.

Reference

Anagnostopoulos G., Androulidakis C., Koukaras E.N., Tsoukleri G., Polyzos I., Parthenios J., Papagelis K., Galiotis C., 2015. Stress Transfer Mechanisms at the Submicron Level for Graphene/ Polymer Systems. ACS Appl. Mater. Interfaces, 7, 4216−4223.

Androulidakis C., Sourlantzis D., Koukaras E.N., Manikas A.C., Galiotis C., 2019. Stress-transfer from polymer substrates to monolayer and few-layer graphenes. Nanoscale Adv., 2019,1, 4972-4980.

Cheng S.J., 2015. Effect of aluminium foil etching process on graphene super capacitor. Chemical Engineering Transactions, 46, 655-660.

Dhand V., Rhee K.Y., Kim H.J., Jung D.H., 2013. A comprehensive review of graphene nanocomposites: research status and trends. Journal of Nanomaterials, 2013, 763953.

Gong L., 2012. Deformation micromechanics of graphene nanocomposites. PhD Thesis, School of Materials, Faculty of Engineering and Physical Sciences, The University of Manchester, Manchester, UK.

Kirilova E., Petrova T., Becker W., Ivanova J., 2019. Mathematical modelling of stresses in graphene polymer nanocomposites under static extension load. 2019 IEEE 14th Nanotechnology Materials and Devices Conference (NMDC), Stockholm, Sweden, October 27-30, 2019, 1-4.

Li Z., Chen Y., Bi C., 2017. Preparation and Properties of Graphene/Nanocopper Reinforced Epoxy Resin Composites. Chemical Engineering Transactions, 60, 103-108.

Loh K. P., Bao Q.L., Ang P.K., Yang J.X., 2010. The chemistry of graphene. Journal of Materials Chemistry, 20, 2277–2289.

Mata T.M., Caetano N.S., Martins A.A., 2015. Sustainability Evaluation of Nanotechnology Processing and Production. Chemical Engineering Transactions, 45, 1969-1974.

Nair R.R., Ren W., Jalil R., Riaz I., Kravets V.G., Britnel L., Blake P., Schedin A.S., Mayorov A.S., Yuan S., Katsnelson M.I., Cheng H.-M., Strupinski W., Bulusheva L.G., Okotrub A.V., Grigorieva I.V., Grigorenko A.N., Novoselov K.S., Geim A.K., 2010. Fluorographene: a two-dimensional counterpart of Teflon. Small, 6(24), 2877–2884.

Novoselov K.S., Jiang D., Schedin F., Booth T.J., Khotkevich V.V., Morozov S.V., Geim A.K., 2005. Two-dimensional atomic crystals. Proc. of National Academy of Sciences of the USA, 102, 10451–10453.

Novoselov K.S., Falko V.I., Colombo L., Gellert P.R., Schwab M.G., Kim K.A., 2012. Roadmap for Graphene. Nature, 490, 192−200.

Petrova T., Kirilova E., Becker W., Ivanova J., 2022. Two-dimensional Stress and strain Analysis for Graphene-polymer Nanocomposite under Axial Load. J. Appl. Comput. Mech., 8(3), 1065–1075.

Rahman R., Haque A., 2013. Molecular modeling of crosslinked graphene–epoxy nanocomposites for characterization of elastic constants and interfacial properties. Composites Part B: Engineering, 54, 353-364.

Thy L.T.M., Cuong P.M., Tu T.H., Nam H.M., Hieu N.H., Phong M.T., 2020. Fabrication of Magnetic Iron Oxide/Graphene Oxide Nanocomposites for Removal of Lead Ions from Water. Chemical Engineering Transactions, 78, 277-282.

Xu C., Xue T., Qiu W., Kang Y., 2016. Size Effect of the Interfacial Mechanical Behaviour of Graphene on a Stretchable Substrate. ACS Appl. Mater. Interfaces, 8 (40), 27099–27106.

Zunita M., Irawantia R., Koesmawati T. A., Lugito G., Wenten G., 2020. Graphene Oxide (GO) Membrane in Removing Heavy Metals from Wastewater: A Review. Chemical Engineering Transactions, 82, 415-420.